High-temperature nucleation and silicide formation at the Co/Si(111)-7×7 interface: A structural investigation

S. A. Chambers, S. B. Anderson,* H. W. Chen, and J. H. Weaver

Department of Chemical Engineering and Materials Science, University of Minnesota, Minneapolis, Minnesota 55455

We have investigated the atomic structure of annealed Co/Si(111) interfaces prepared by the evaporation of one-, two-, and thirty-monolayer equivalent coverages of Co. Experimental and theoretical angular distributions of the Co LMM Auger intensity reveal that for all coverages investigated a $CoSi_2$ phase forms which is rotated 180° about the surface normal relative to the substrate. At low coverages, the $CoSi_2$ phase is in the form of clusters which appear to be two to three $CoSi_2$ layers in thickness and are terminated by a Si(111) bilayer. The Si(111) overlayer, which is in addition to the terminal plane of Si atoms associated with the outermost $CoSi_2$ layer, also appears to be rotated 180° about the surface normal relative to the Si substrate.

I. INTRODUCTION

Silicide-Si(111) interfaces involving the near-noble metals Co and Ni have been shown to be abrupt and epitaxial when grown by either metal deposition onto a heated Si substrate or by annealing the interface grown at room temperature.[1-4] This result is expected in light of the close lattice match between the metal silicides and Si. For Co and Ni, the disilicide forms with a calcium fluoride crystal structure and lattice constants of 5.356 Å and 5.406 Å, respectively. Comparison with the Si lattice constant of 5.428 Å shows the mismatch to be 1.3% for $CoSi_2$ and 0.4% for $NiSi_2$. Thus these systems constitute ideal choices for fundamental studies of epitaxial growth and lateral homogeneity in thin silicide films. Moreover, abruptness and epitaxy at a silicide-Si interface make possible the formation of epitaxial heterostructures of the type Si/MSi_2/Si, where M=Co or Ni.[5]

Cross-sectional transmission electron microscopy (TEM) measurements have shown that a deposition of a few hundred angstroms of Co onto room-temperature Si(111), followed by annealing at 800–950 °C, results in the formation of an epitaxial $CoSi_2$ phase which is rotated 180° about the surface normal with respect to the substrate (the so-called B-type silicides). This result is corroborated by extended electron-energy-loss fine-structure measurements in which silicide phases grown in the same way yield a Co nearest-neighbor distance which is (within experimental error) that expected for $CoSi_2$.[6] In these experiments emphasis was placed on the structure of the extended interface, which is of the order of 100 Å thick.

In this paper we examine the atomic structure for ultrathin $CoSi_2$/Si(111) interfaces. Such studies are of vital importance because atoms in the interfacial layer constitute the template for further crystal growth. We have exploited the intensity anisotropies associated with Co LMM Auger emission from a one-monolayer-equivalent deposition of Co on room-temperature Si(111)-7×7, which was subsequently annealed at 500 °C. Comparison of the associated angular distributions with those for the extended B-type $CoSi_2$ phase, as well as those generated by kinematical scattering calculations, permits us to determine the structure and morphology of the ultrathin interfacial layer. This technique has been shown to be a useful tool for structural determination of metal-semiconductor[7] and metal-metal interfaces.[8-10]

II. EXPERIMENTAL AND COMPUTATIONAL DETAILS

All measurements were performed on a spectrometer described in detail elsewhere,[11] with the exception of the following modifications. A second electron gun made by Kimball Physics (KP) capable of beam energies up to 10 keV has been added to complement the 5-keV gun built into the cylindrical mirror analyzer (CMA). The angle of incidence of the KP gun is 20° with respect to the polar axis of rotation, in contrast to the CMA gun for which the angle of incidence is 90°. The higher incident energies afforded by the new gun yield better Auger cross sections for deep core-core-core transitions in which the binding energy of the initially ionized core level is of the order of a few keV or more.[12]

In addition, a Digital Equipment Corporation PDP11/23 microcomputer has been incorporated for data acquisition and analysis, replacing the multichannel analyzer used in earlier studies. Auger intensities were determined by Shirley or S-shaped background subtraction[13] and integration following a single 11-point smooth procedure. To ensure that intensities were not affected by variations in incident-beam current, each integrated area was normalized by dividing by the number of counts in an arbitrary channel on the high-kinetic-energy side of the peak of interest. Comparison with angular distributions obtained without normalization in which the primary beam current was carefully monitored throughout the experiment showed that this procedure did not alter the angular distributions in any significant way.

A p-type Si wafer cut and polished to within 1° of the (111) plane was chemically etched, lightly argon-ion sput-

tered and annealed at 950 °C under ultrahigh vacuum (UHV) conditions to produce the 7×7 reconstruction. Polar-angle alignment was done with a He-Ne laser once the sample was mounted on the goniometer but before being placed in the vacuum system. Once under UHV $(5\times10^{-11}$ Torr), further alignment of both polar and azimuthal directions was done by finding maxima in the (11) and (10) low-energy electron diffraction (LEED) beams and in the Si KLL Auger intensity. Arbitrarily defining $\phi=0°$ as the [$\bar{2}11$] direction in the plane of the surface, the Si KLL intensity locally maximizes at a polar or collection angle (θ) of 54° with respect to the surface and an azimuthal angle (ϕ) of 0° (the [011] direction). Local maxima along low-index directions results from forward focusing of the outgoing wave.[11,14−17] This azimuthal angle calibration procedure was verified by finding the (11) and (10) LEED beams, produced by the CMA electron gun at an incident energy of 34 eV, which maximize at $\phi=0°$ and 60°, respectively. These two alignment procedures agreed to $\pm1°$.

Evaporation of Co was done from a W coil and was monitored with a quartz-crystal oscillator. During evaporation, the system pressure rose to $\sim5\times10^{-10}$ Torr but quickly recovered to the operating value of $\sim5\times10^{-11}$ once the evaporator was shut off. Subsequent annealing to temperatures of 500–600 °C was monitored with a thermocouple-calibrated infrared pyrometer. All Co LMM spectra were obtained with a primary beam energy of either 5 or 6 keV and a primary current of less than 0.5 μA. Si KLL spectra used for alignment purposes were obtained at 10 keV. Each angular distribution reported here is based on several different scans which sampled different portions of the crystal and utilized the two different electron guns.

Kinematical scattering calculations[17] were performed on a VAX 11/780 computer. The surface was modeled as a cluster of atoms with a lateral dimension of $7a\times7a$, where a is the dimension of the surface unit cell, and a depth of three to seven layers. This choice of cluster size was found to yield fully convergent results. In each layer the emitting Co atom was chosen to be in the geometric center of the lateral plane. The lattice constant in the $CoSi_2$ layer was taken to be the same as that of the substrate Si.

Atomic scattering factors were taken from calculations by Fink and Ingram[18] and Gregory and Fink.[19] Quadratic interpolations over energy for both Co and Si and over atomic number for Si were performed to arrive at scattering factors and phase shifts for Si and Co atoms scattering an incident electron plane wave at the kinetic energy of Co LMM emission, 771 eV. The resultant scattering factors were then reduced by a factor of 2 to compensate for the use of free-atom values as opposed to more appropriate muffin-tin scattering factors and for spherical-wave effects, which have been shown to be important in high-energy forward scattering such as we observe in the present work.[20] An inner potential of 15 eV, which is intermediate between that for bulk Si and bulk Co, was chosen to be representative of the Co/Si interface. An inelastic mean free path of 15 Å, computed from empirical equations by Seah and Dench, was used for Co LMM

emission.[21] Lattice vibrations were accounted for using Debye-Waller factors based on published Debye temperatures.[22]

III. RESULTS

Following the suggestion of Derrien,[23] we have performed calculations for a number of different structures which could be put into four fundamental categories: (i) $CoSi_2(111)$ in which the [011] direction is parallel to that found in the substrate (the "type-A" silicide) and Si atoms associated with the interfacial $CoSi_2$ layers are bound to Si atoms in the terminal substrate plane; (ii) type-A silicide in which Co atoms in the interfacial $CoSi_2$ layer are bound to Si atoms in the terminal substrate plane, (iii) $CoSi_2(111)$ in which the [011] direction is rotated 180° about the surface normal relative to that found in the substrate (the "type-B" silicide) and Si atoms associated with the $CoSi_2$ layer are bound to Si atoms in the terminal substrate plane; and (iv) type-B $CoSi_2$ in which Co atoms in the interfacial $CoSi_2$ layer are bound to Si atoms in the terminal substrate plane. Side views of these four crystal structures are shown in the top half of Fig. 1. Note that Co atoms in the interfacial layer are sevenfold coordinated in structures (i) and (iii), but fivefold in (ii) and (iv). Co is eightfold coordinated in bulk $CoSi_2$.

These four structures are expected to yield different Co LMM Auger diffraction profiles, with extensive differences expected between type-A and type-B silicides. It is known from TEM studies that the extended $CoSi_2$ phase grown on Si(111)-7×7 is of the B type structure.[3] Therefore, we have measured Co LMM polar intensity profiles on the interface prepared by evaporating 30 monolayers (ML) of Co and annealing at 700 °C for 5 min, as shown in the top of each plane in Fig. 2. Because of the symmetry of the (111) orientation of $CoSi_2$, a 60° rotation about the surface normal is equivalent to a 180° rotation. Therefore we have in these profiles a structural fingerprint of epitaxial B-type $CoSi_2$. Major peaks along internuclear vectors are observed due to the forward-peaking nature of electron-atom scattering at the kinetic energy of Co LMM emission.[11,14−17] For example, maxima are found along
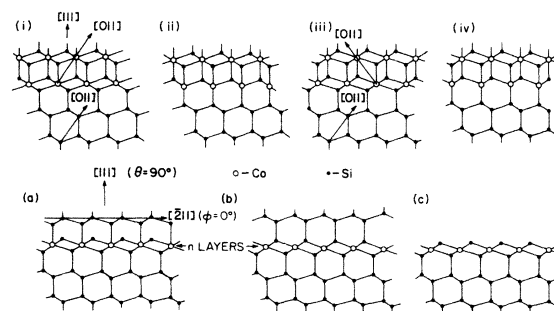
FIG. 1. Top panel: side view of four structural models of the $CoSi_2/Si(111)$ interface. Bottom panel: n-layer analogs of bulk structure (iii) in the top panel for which kinematical scattering calculations were performed.

[011] and [111] directions, as shown in Fig. 2(a). Also shown in Fig. 2 are polar profiles for 1- and 2-ML coverages annealed at 500 °C for 2 min. All features found in the 30-ML data are seen in the data at lower coverages, although there are differences in relative intensities, particularly at $\phi = 0°$. The features at $\theta = 68°$ and 90° grow in intensity relative to those at 56°, 35°, and 16° as additional Co is added. However, it seems clear that for ultrathin coverages (1–2 ML), the CoSi$_2$ that forms is of B-type structure.

To determine details of the silicide structure, we have performed additional measurements for a 1-ML initial coverage and a number of calculations involving different arrangements of a 1-ML equivalent (7.8×10^{14} atoms/cm^2) of Co in the form of B-type CoSi$_2$. For the purpose of our calculations, we have modeled ultrathin analogs of
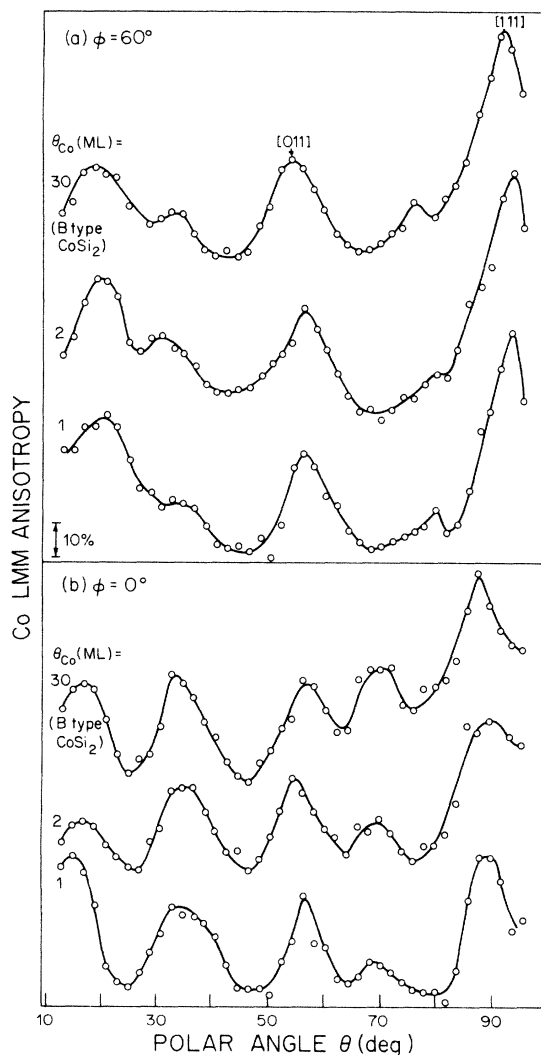
FIG. 2. Experimental Co LMM polar angular distributions in two different high-symmetry azimuthal planes. The azimuthal angle ϕ is defined with respect to the [$\bar{2}$11] direction in the plane of the surface. Measurements were made for 1, 2, and 30 monolayer equivalents of Co which were subsequently annealed to form CoSi$_2$. Intensity variations are defined in terms of anisotropy, which is given by [$(I_{max} - I_{min})/I_{max}$] × 100.

these four bulk structures for comparison with experiment. Because of the symmetry of the (111) orientation of CoSi$_2$, an azimuthal angular distribution for a B-type structure can be transformed into that for an A-type structure simply by phase shifting the data by 60°. We have exploited this fact to verify that the annealed 1-ML CoSi$_2$(111)/Si(111) interface is of B-type crystal structure, as suggested by the data in Fig. 2. Thus we eliminate from further consideration structures (i) and (ii) in Fig. 1, as discussed in the next paragraph. Unfortunately, we have found that calculated angular distributions for geometries (iii) and (iv) are virtually identical, precluding the possibility of distinguishing between the two modes of bonding to the substrate. The physical reason for this result is that high-energy Auger electron diffraction only probes structure in the forward path of the outgoing electron due to the forward peaking of electron-atom scattering in the high-energy regime.[24] However, we believe that geometry (iii) is more likely to be correct inasmuch as Co atoms in the interfacial layer can achieve a coordination number of 7, which is closer to the bulk value of 8. In contrast, interfacial Co atoms in geometry (iv) can achieve a coordination number of only 5. Therefore we have chosen to model in detail three ultrathin analogs of bulk structure (iii), which are shown in the bottom half of Fig. 1 as (a), (b), and (c). Structure (c) is simply n layers of B-type CoSi$_2$(111) on Si(111) which is Si terminated and in which the Co coordination number is 6. Structures (a) and (b) are n layers of B-type CoSi$_2$(111) on Si(111) with a surface bilayer of Si(111). The only difference between (a) and (b) is the orientation of the Si bilayer; in (a) the Si layer is rotated 180° about the surface normal relative to the Si substrate whereas in (b) it is not.

In Fig. 3 we show measured and calculated Co LMM polar scans at $\phi = 60°$ for 1 ML of Co annealed for 2 min at 500 °C. The labels (a), (b), and (c) correspond to the structural models shown in Fig. 1 and n is the number of layers of CoSi$_2$ which are assumed to form on Si(111). Inasmuch as 1 ML of as-deposited Co would give rise to one continuous layer of CoSi$_2$ if the chemistry so permitted, multiple layers (i.e., $n > 1$) correspond to the modeling of CoSi$_2$ clusters. As can be seen, agreement between theory and experiment is quite good for model (a) with either one, two, or three layers of CoSi$_2$. The three major features at 16°, 54°, and 90° as well as the weak features at 33° and 75° are well reproduced, although the peak at 16° is somewhat too weak for $n = 3$. The agreement for model (b) is slightly poorer. Specifically, the weak feature at 33° is not accounted for and the intensities of the features at 16° and 54° are not as similar to experiment as those for model (a). Model (c) does not reproduce the experimental data particularly well for either $n = 1$ or $n = 2$. For $n = 2$, the features at 54° and 90° are somewhat too weak, while the peak at 16° is too strong. For $n = 1$, the peaks at 54° and 90° are missing altogether. These results then suggest that the B-type silicide is sandwiched between the substrate and a bilayer of Si(111). However, the number of layers of silicide and the orientation of the Si bilayers cannot be determined from the results of Fig. 3 alone.

In Fig. 4 we present analogous data for $\phi = 0$. Model (c) with $n = 1$ can again be eliminated from further con-

sideration as there is no resemblance between theory and experiment. Moreover, we can probably rule out one-layer compounds of structures (a) and (b). In both cases, the peak at 54° is too weak, and for model (b) with $n=1$, the feature at 35° is too large relative to others in the profile. Reasonable agreement is obtained with two or three layer clusters of structures (a) and (b), although in all three cases the peak at 15° is too small and the peak at 90° is too large. Fair agreement is also obtained for model (c) with $n=2$, although a doublet appears at 35°, compared to a singlet in the experimental data. Taken together, the polar profiles indicate that the interface is composed of B-type clusters, two to three layers deep. For further insight, we now turn to azimuthal profiles taken over a wide range of polar angles.

In Fig. 5 we show a set of measured and calculated Co LMM azimuthal angular distributions for a polar angle (θ) of 14° relative to the surface. In both theory and experiment, major diffraction features appear at 0°, 60°, and 120°, with the one at 60° clearly being the largest. Much smaller features occur in the valleys between 0° and 60° and between 60° and 120°, and there is symmetry about the mirror plane at 60°. That the $CoSi_2$ is B-type is clearly seen by recalling that the calculated angular distributions for analogous A-type structures (not shown) look exactly like those in Fig. 5, only with a 60° phase shift. Thus for an A-type structure the large diffraction feature would appear at 0° and 120° and the smaller feature would be at 60°. The strong similarities between the angular distributions for the three models simply reflect the fact that at $\theta=14°$ the outgoing Co LMM electron does not strongly interact with atoms outside the layer containing the emitter. As was shown in the case of Cu/Si(111), Auger electron diffraction is strictly a local structural probe with prominent scattering occurring only at nearest- and next-nearest-neighbor sites.[7] At $\theta=14°$, the primary interac-

FIG. 3. Experimental and theoretical Co LMM polar profiles at $\phi=60°$ for 1 ML of Co annealed for two minutes at 500 °C. (a), (b), and (c) refer to the structural models found in Fig. 1.
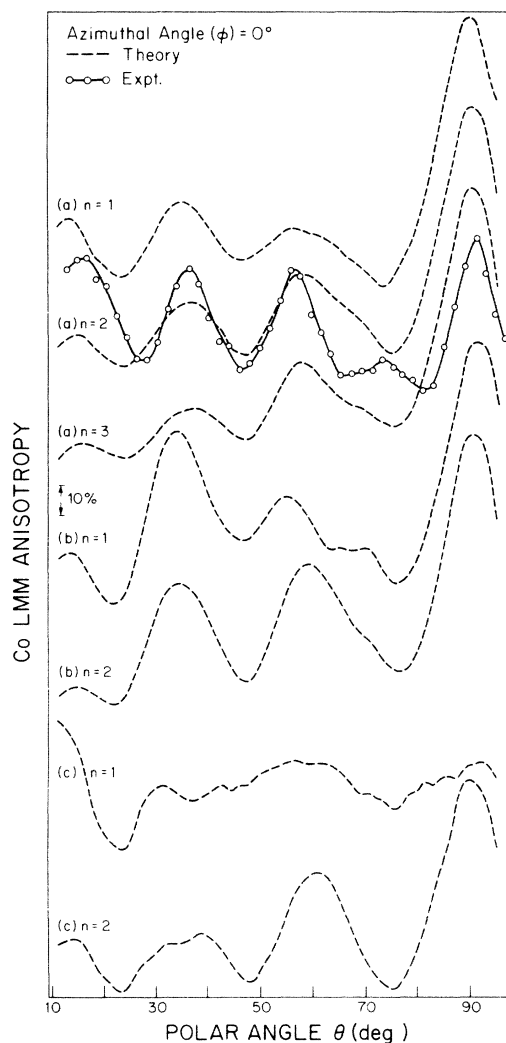
FIG. 4. Same as Fig. 2 for $\phi=0°$.

tion of the Co *LMM* electron is with near-neighbor Si and Co atoms in the immediate $CoSi_2$ layer. The excellent agreement between theory and experiment supports the $CoSi_2$ structural model used in geometries (a), (b), and (c) (*B*-type $CoSi_2$). In order to sample any structure above the $CoSi_2$ layers, we must make measurements at higher polar angles.

In Fig. 6 we show azimuthal scans for $\theta = 36°$. At this collection angle the number of layers of $CoSi_2$ in the cluster begins to affect the calculated angular distributions. Specifically, only those angular distributions based on models with more than one layer of $CoSi_2$ bear a resemblance to experiment. Of the four with $n > 1$, model (a) with $n = 2$ or 3 agrees best. All features generated by the calculation are present in the experimental data and the intensities are nearly correct. On the other hand, the doublets at $\phi = 30°$ and $90°$ are predicted to be somewhat too weak for model (b) with $n = 2$. Furthermore, the valleys at $10°$ and $110°$ are too shallow for model (c) with $n = 2$. For all one-layer structures, there are major qualitative differences between theory and experiment.

In Fig. 7 we present theory and experiment for azimuthal scans at $\theta = 54°$, which includes the [011] direction in the $CoSi_2$ at $\phi = 60°$. As in Fig. 6, the multilayer

structural models generate the best agreement with experiment. Models (a) with $n = 2$ and 3 and (b) with $n = 2$ are essentially the same. All three predict major features at $\phi = 0°$, $60°$, and $120°$ with the peak at $60°$ being the largest. Much weaker features are predicted at $20°$ and $100°$. Model (c) with $n = 2$ shows the same structure only with a smaller difference in intensity between the feature at $60°$ and those at $0°$ and $120°$. The experimental profile shows large but equal-size peaks at $0°$, $60°$, and $120°$ and weak features at $17°$ and $100°$, in good agreement with all four multilayer structural models. Single-layer models (a) and (b) predict features at $0°$ and $120°$ which are slightly too low and model (c) with $n = 1$ fails to generate the peak at $60°$. From the data, we gain additional evidence that $CoSi_2$ forms in clusters rather than as a continuous monolayer, but we cannot determine the details of the surface termination. In order to do so, we must collect azimuthal angular distributions at a higher polar angle at which outgoing Co *LMM* Auger electrons scatter from atoms in the terminal plane.

In Fig. 8 azimuthal scans at $\theta = 70°$ are shown. At this high polar angle, we effectively probe the surface layer, as evidenced by the significant differences between models
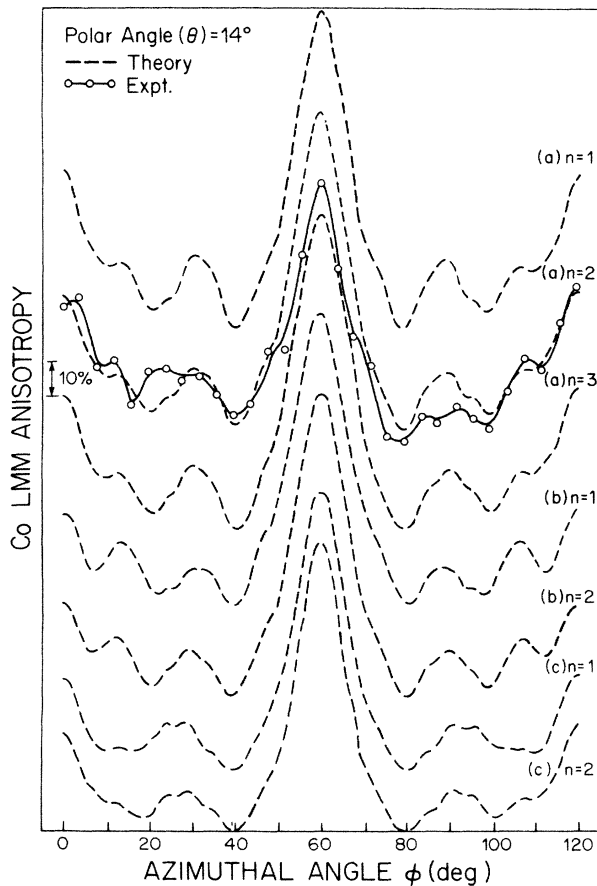
FIG. 5. Experimental and theoretical Co *LMM* azimuthal profiles at $\theta = 14°$ for the annealed 1-ML Co/Si(111) interface.
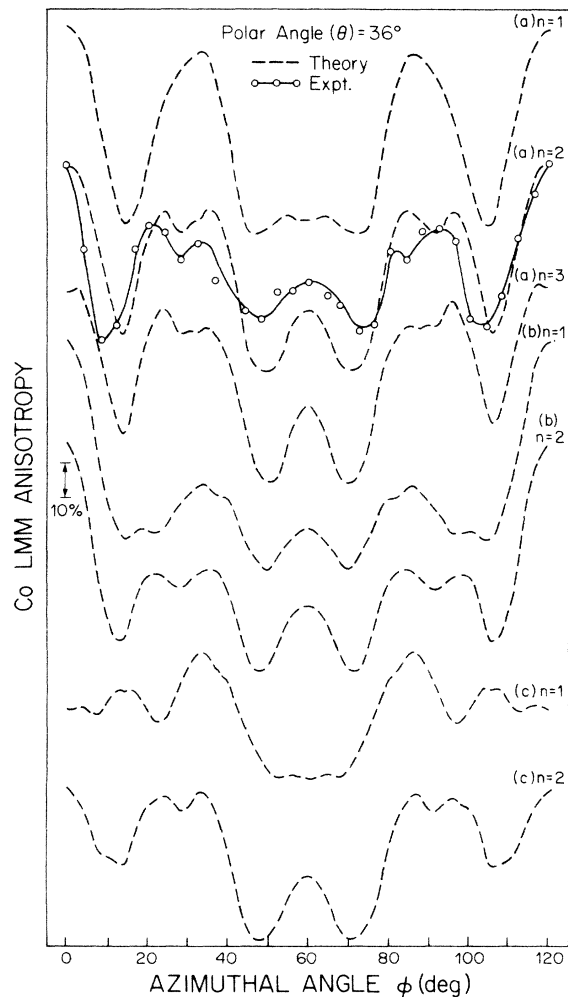
FIG. 6. Same as Fig. 5 for $\theta = 36°$.

(a), (b), and (c) for a fixed value of n. For example, agreement between theory for $n=2$ and experiment is excellent for model (a), but only marginal for (b) and quite poor for (c). As in previous cases, model (a) with $n=2$ and 3 are similar. Again, the one-monolayer structures fail to reproduce the experimental data and can be ruled out. Of all the angular distributions collected, this one shows the largest differences between the different structural models investigated. The best fit is for model (a) with $n=2$ or 3.

Summarizing, azimuthal scans at $\theta=14°$, $36°$, and $54°$ and polar scans at $\phi=0°$ and $60°$ show that a number of the proposed B-type structures agree well with experiment. However, the azimuthal scan at $\theta=70°$ enables us to conclude that model (a) with two or three layers of CoSi$_2$ is the most plausible for the interface. One obvious advantage of model (a) is that the surface Si bilayer is oriented so that Co atoms in the terminal CoSi$_2$ plane will be coordinated in the same way as they are in bulk CoSi$_2$.

IV. DISCUSSION

A. Comparison with other investigations of NiSi$_2$/Si(111) and CoSi$_2$/Si(111)

Investigation of annealed ultrathin Ni layers on Si(111) by medium-energy ion scattering (MEIS) indicates that
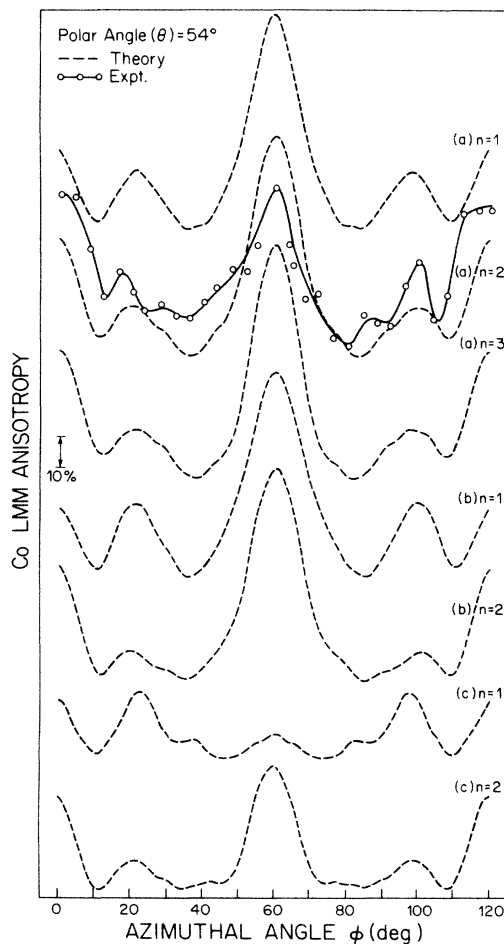
FIG. 7. Same as Fig. 5 for $\theta=54°$.
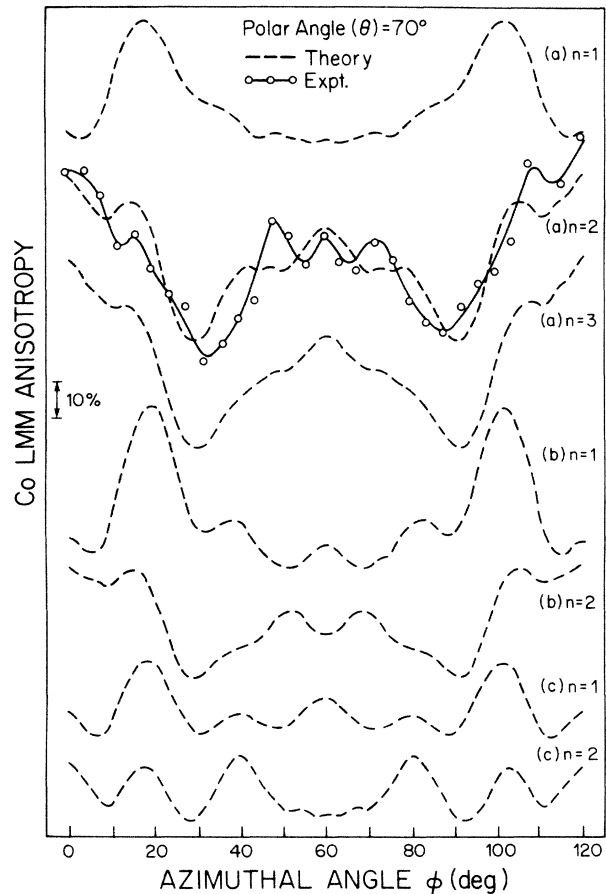
FIG. 8. Same as Fig. 5 for $\theta=70°$.

for coverages of ~ 6 ML or less the silicide forms clusters.[25] This conclusion is based on the width of the Ni peak in the He ion scattering spectrum. For coverages as low as ~ 2 ML, ion scattering angular distributions indicate that the silicide is of B-type structure with a minimum thickness of four NiSi$_2$ layers. Thus, it appears that the dynamics of reaction at elevated temperature are the same for CoSi$_2$ and NiSi$_2$ on Si(111).

The atomic structure of the NiSi$_2$/Si(111) system have also been studied by LEED intensity analysis.[26] It is found that for nominal coverages of 6 ML or less, the LEED I-V curves for several diffracted beams are essentially identical to those of quenched Si(111)-1$\times$1. This result is consistent with the formation of islands at very low coverages, leaving areas of "bare" Si(111) with dimensions of the order of the coherence length of the LEED incident beam or larger. However, thicker NiSi$_2$ phases exhibit LEED spectra which agree well with dynamical scattering calculations in which the surface is modeled as Si-terminated NiSi$_2$ with a 25% contraction of the first interlayer spacing. It appears, therefore, that the terminal Si(111) bilayer suggested by the present work for the CoSi$_2$/Si(111) interface does not form on the NiSi$_2$/Si(111) interface. Subsequent LEED work in which Si was evaporated onto NiSi$_2$/Si(111) and annealed at successively higher temperatures indicates that I-V curves characteristic of quenched Si(111)-1$\times$1 give way to those

observed for NiSi$_2$(111) as the annealing progresses.[27] In the middle of the heat treatment, the LEED *I-V* curves closely resemble those obtained by averaging curves for Si(111)-1×1 and NiSi$_2$(111), suggesting that the removal of Si by thermal agitation leaves behind Si islands and patches of NiSi$_2$. Interestingly, the LEED spectra for evaporated Si were consistently the same as those of the Si substrate, regardless of whether the NiSi$_2$ was of *A*- or *B*-type structure.

Pirri et al.[28] have performed LEED, x-ray photoemission spectroscopy, angle-resolved ultraviolet photoemission, and work-function measurements on a CoSi$_2$(111)/ Si(111) surface with Co deposited onto the silicide and subsequently annealed. Their work showed that the spectral properties of 1 ML of Co deposited onto 100 Å of CoSi$_2$(111) are substantially different from those of the original Si-rich CoSi$_2$ surface. However, annealing at 420 °C converts the surface spectral properties back to those of Co-rich CoSi$_2$. Thus a *new* layer of CoSi$_2$ has been formed. The issue is where did the Si necessary to form the new layer of silicide come from? The nearly perfect epitaxy in the CoSi$_2$ phase demonstrated by TEM measurements[3] diminishes the probability of Si diffusion from the substrate through grain boundaries. Furthermore, Pirri et al. found that the Co(2p)/Si(2s) XPS intensity ratio did not change as a result of annealing at temperatures up to ~450°, suggesting that Si outdiffusion did not occur. The presence of 2 ML of Si on the surface of the CoSi$_2$ would make possible the formation of a new layer of CoSi$_2$ with minimal atomic diffusion.

B. Comparison with noble metal—Si(111) interfaces

The annealed 1—2 ML *M*/Si(111) interfaces, where *M* = Ni, Co, Cu, and Ag, have been studied by structurally sensitive techniques. These results point out some interesting differences between interfaces formed with near-noble versus noble metals. As discussed here, 1—2 monolayer equivalents of Ni and Co transform to three-dimensional *B*-type *M*Si$_2$ clusters upon annealing. In contrast, 1 ML of Cu (Ref. 7) or Ag (Ref. 29—32) on Si(111) results in a continuous, ordered two-dimensional structure in which the metal atoms occupy hollow sites and induce a reconstruction.

The structure of the annealed interface is critically dependent on the interaction of the metal atoms with the semiconductor surface at room temperature. Extended x-ray-absorption fine-structure[33] (EXAFS) measurements and MEIS (Ref. 34) showed that Ni reacts at very low

coverages (1—2 ML) with Si(111) to form silicide clusters at room temperature, although different conclusions were reached about the stoichiometry of the reacted phase with the two techniques. High-resolution synchrotron-radiation photoemission and high-resolution electron-energy-loss spectroscopy measurements for the Cu/Si(111) interface indicate that Cu forms inert clusters up to ~3 ML and that intermixing does not occur until this threshold coverage is exceeded.[35] Thus when interaction with the substrate is strong and stable silicide clusters form (Ni and Co), annealing will drive the silicide formation reaction to completion, leaving the product in the form of clusters. In contrast, when interaction with the substrate is weak (Cu and Ag), annealing causes the dispersion of adatoms across the surface and the occupation of energetically favorable hollow sites. The final result is a continuous two-dimensional structure.

V. CONCLUSION

We have probed the structure of the annealed 1-, 2-, and 30-ML Co/Si(111)-7×7 interface with Auger electron diffraction and related kinematical scattering calculations. Angular distributions for the 1- and 2-ML interfaces are essentially the same as those for the 30-ML interface, which is known by TEM to form *B*-type CoSi$_2$ when annealed. For the 1-ML case, we find that optimal agreement between theory and experiment occurs when we assume that Co converts to CoSi$_2$(111) clusters ~2—3 layers thick which are terminated by a Si(111) bilayer. The technique is very sensitive to the orientation of the CoSi$_2$ clusters relative to the substrate, with agreement occurring only for a *B*-type orientation. The method is also sensitive to the presence of the Si(111) bilayer, although the precise positions of the atoms within the bilayer are not so easy to identify. However, superior agreement with experiment occurs when the Si(111) bilayer is of the opposite orientation to that of the substrate.

ACKNOWLEDGMENTS

---

*Also at Department of Physics, Bethel College, St. Paul, MN 55112.

[1] R. T. Tung, J. M. Gibson, and J. M. Poate, Phys. Rev. Lett. **50**, 429 (1983).

[2] R. T. Tung, J. C. Bean, J. M. Gibson, J. M. Poate, and D. C. Jacobson, Appl. Phys. Lett. **40**, 684 (1982).

[3] J. M. Gibson, J. C. Bean, J. M. Poate, and R. T. Tung, Appl. Phys. Lett. **41**, 818 (1982).

[4] M. Liehr, P. E. Schmid, F. K. LeGoues, and P. S. Ho, Phys. Rev. Lett. **54**, 2139 (1985).

[5] J. C. Hensel, R. T. Tung, J. M. Poate, and F. C. Unterwald, Phys. Rev. Lett. **54**, 1840 (1985); Appl. Phys. Lett. **47**, 151 (1985).

[6] E. Chainet, M. De Crescenzi, J. Derrien, T. T. A. Nguyen, and R. C. Cinti, Surf. Sci. **168**, 801 (1986).

[7] S. A. Chambers, S. B. Anderson, and J. H. Weaver, Phys. Rev.

B 32, 581 (1985).

[8]W. F. Egelhoff, Jr., J. Vac. Sci. Technol. A2, 350 (1984).

[9]E. L. Bullock and C. S. Fadley, Phys. Rev. B 31, 1212 (1985).

[10]S. A. Chambers, S. B. Anderson, and J. H. Weaver, Phys. Rev. B 32, 4872 (1985).

[11]S. A. Chambers and L. W. Swanson, Surf. Sci. 131, 385 (1983).

[12]S. Mroczkowski and D. Lichtman, J. Vac. Sci. Technol. A 3, 1860 (1985).

[13]D. A. Shirley, Phys. Rev. B 5, 4709 (1972).

[14]S. Kono, C. S. Fadley, N. F. T. Hall, and Z. Hussain, Phys. Rev. Lett. 41, 117 (1978).

[15]L.-G. Petersson, S. Kono, N. F. T. Hall, C. S. Fadley, and J. B. Pendry, Phys. Rev. Lett. 42, 1545 (1979).

[16]W. F. Egelhoff, Jr., Phys. Rev. B 30, 1052 (1984).

[17]C. S. Fadley, in *Progress in Surface Science,* edited by S. G. Davison (Pergamon, New York, 1984), Vol. 16, p. 275.

[18]M. Fink and J. Ingram, At. Data 4, 129 (1972).

[19]H. Gregory and M. Fink, At. Data Nucl. Data Tables 14, 39 (1974).

[20]M. Sagurton, E. L. Bullock, R. Saiki, A. Kaduwela, C. R. Brundle, C. S. Fadley, and J. J. Rehr, Phys. Rev. B 33, 2207 (1986).

[21]M. P. Seah and W. A. Dench, Surf. Int. Anal. 1, 2 (1979).

[22]N. W. Ashcroft and N. D. Mermin, *Solid State Physics* (Holt, Rinehart, and Winston, New York, 1976), p. 461.

[23]J. Derrien, Surf. Sci. 168, 171 (1986).

[24]The forward focusing of scattered electron intensity at high kinetic energies is easily appreciated by examining tables of pubilshed scattering factors as those found in Refs. 14 and 15.

[25]E. J. van Loenen, A. E. M. J. Fischer, J. F. van der Veen, and F. Legous, Surf. Sci. (to be published).

[26]W. S. Yang, F. Jona, P. M. Marcus, Phys. Rev. B 28, 7377 (1983).

[27]S. C. Wu, Y. S. Li, F. Jona, and P. M. Marcus, Phys. Rev. B 32, 6956 (1985)

[28]C. Pirri, J. C. Peruchetti, D. Bolmont, and G. Gewinner, Phys. Rev. B 33, 4108 (1986).

[29]Y. Terada, T. Yoshizuka, K. Oura, and T. Hanawa, Surf. Sci. 114, 65 (1982).

[30]J. Stöhr, R. Jaeger, G. Rosi, T. Kendelewicz, and I. Lindau, Surf. Sci. 134, 813 (1983).

[31]S. Kono, H. Sakurai, K. Higashiyama, and T. Sagawa, Surf. Sci. 130, L299 (1983).

[32]M. Aono, R. Souda, O. Oshima, and Y. Ishizawa, Surf. Sci. 168, 713 (1986).

[33]F. Comin, J. E. Rowe, and P. H. Citrin, Phys. Rev. Lett. 51, 2402 (1983).

[34]E. J. van Loenen, J. W. M. Frenken, and J. F. van der Veen, Appl. Phys. Lett. 45, 41 (1984).

[35]S. A. Chambers, M. del Giudice, M. W. Ruckman, S. B. Anderson, J. H. Weaver, and G. J. Lapeyre, J. Vac. Sci. Technol. (to be published).